ISSN 2286-4822
www.euacademic.org

EUROPEAN ACADEMIC RESEARCH
Vol. II, Issue 2/ May 2014

Impact Factor: 3.1 (UIF)
DRJI Value: 5.9 (B+)

Production of Liquefied Natural Gas Using Radioactive Waste and Agricultural Residue

MOHAMMED NSAIF ABBAS
Environmental Engineering Department
College of Engineering
The University of Mustansiriyah
Baghdad, Iraq

Abstract:

The goal of this study is to appraise the effectiveness of the rice husk (RH) as low cost material for removing cesium, from aqueous solution and try to utilization from remaining samples in benefit method. Analysis of the respective rate data in accordance with five kinetic models is applied. The results show that the maximum adsorption was observed in alkaline condition, using 50g of adsorbent for 1 mg.l^{-1}of radioactive liquid waste at 45°C, in 1h of residential time and 5 ml.min^{-1} for fixed bed experiments, while for batch experiments the Langmuir model was the best. The higher percent removal was 95.70 % for cesium at initial cesium concentration of 1 mg/l. The kinetic and thermodynamic parameters at different temperatures were tested. The experimental data were fitted well by the pseudo-second-order kinetic model. The free energy (ΔG), enthalpy (ΔH), entropy (ΔS) and activation energy (Ea) of the adsorption were calculated. These parameters showed that the sorption of ^{137}Cs onto RH was spontaneous and endothermic in nature. The samples of RH remaining were segregate and try to utilization from it in synthesis of promoted type Y-zeolite catalyst in process of n-heptane catalytic cracking. The results show that the synthesis catalyst gives good conversion of n-heptane to liquefied natural gas (propane and butane) than normal type Y-zeolite catalyst.

Key words: Cesium, adsorption, agriculture residue, liquefied natural gas.

1. Introduction

Cesium is one of alkaline, radioactive and rare comparatively element exists in the nature fundamentally by erosion and weathering of rocks and minerals (Ghaffar *et. al.*, 2012). It is predestined to about approximately 3 ppm in the Earth's crust. Cesium is existed in the liquid phase and crystallizes last. Therefore, the largest sediment of cesium is zone pegmatite ore resources formed by fructify process (Turekian, and Wedepohl, 1961). The Dutch scientist, Bunsen and Kirchhoff, disclosed cesium in 1860 using the newly sophisticated flame spectroscopy process. Because of its bright blue emission spectrum, they selected a name originated from the Latin word *caesius*, meaning sky-blue. (Coplen, and Peiser, 1998). Cesium salts are used to fortified many glass types. Cesium nitrate is used to manufacture optical glasses. Sometimes it is used to eliminate traces of oxygen from the vacuum tubes and from light bulbs. In photoelectric cells, in increasing the sensitivity of electron tubes and in optical instruments cesium is used in chloride form.

Cesium is used also in atomic clocks and lastly in ion propulsion process. It is used as a catalyst promoter for many reactions in industry; consolidating the function of other metal oxides in the capacity and for the hydrogenation of organic compounds. It is sent out to the air, water and soil by effluents of industries, treating ores. Due to these activities, different wastes containing various radioactive isotopes and ions of cesium were created pollution of the water resources like rivers, lakes or ground water (Sasaki *et. al.*, 2013). Large quantities of nuclear wastes are generated from reprocessing of nuclear fuel and charged particle accelerators due to operation of large number of nuclear power plants. These nuclear wastes are often underground buried in stainless steel containers. Toxic radioactive materials may be transferred to the surrounding soil and groundwater as a result to the probability seepage of some of these containers even in distant future (Danilin and Drozhzhin, 2007). Also, these radionuclides pollutants my prevalence to the surrounding due to tests of nuclear weapon, nuclear episode such as Chernobyl nuclear power plant disaster in 26 April 1986, forbidden discharge or puffs and the possible influx of certain toxic industrial effluents (Al Hamarneh *et. al.*, 2003; Onishi, 2014). Amongst these, ^{137}Cs is which is created mainly as a nuclear fission product. It is one of the main and common radioactive elements with a half-life of 30.17 years which emit beta particles and relatively strong gamma radiation when it undergoes radioactive decay (Yavari *et. al.*, 2011).

Cesium is caused many risks to both the environment and human health; due to the wide solubility of cesium compounds in water. The high solubility of cesium results in its transfer from surface water to groundwater. Because it's yield in nuclear power plants in high rates, having long half-lives (half-life of ^{135}Cs is 2.3×10^{6} years, ^{137}Cs is 30 years and ^{134}Cs is 2 years) and its high solubility in aqueous solutions, all these reasons cause its dangerous effects (Cortés-Martínez *et. al.*, 2010). When ^{137}Cs enters into the organism, it allows the radioactive material to be dispersed throughout the body with higher concentration in muscle tissues and lower concentration in bones. Therefore it can increase the cancer risk. Exposure of human to cesium through breathing, drinking or eating digest, diarrhoea, nausea, hyperirritability, vomiting, spasms and bleeding may be result and if exposure continues for a long time people may be lose consciousness.

Finally coma or even death may carry out (ATSDR, 2004). Therefore, the elimination and disconnection of ^{137}Cs from radioactive waste solution in economical and safe methods has been paid serious solicitude. Different methods have been applied to remove ^{137}Cs from aqueous solution such as precipitation (Rogers *et. al.*, 2012), extraction (Inoue *et. al.*, 2014), ion exchange (Pátzay *et. al.*, 2009), bioaccumulation

(Rowan, 2013), electric-field assisted (Sviridov *et. al.*, 2012) techniques and adsorption (Yavari *et. al.*, 2011). Among them, adsorption technique is one of the most commonly and efficacious methods in radioactive waste treatment and it represented the green chemistry direction to reduce the use of toxic and carcinogenic solvents in remediation processes of wastewater (Cortés-Martínez *et. al.*, 2010; Bernatskii and Pavlov, 2010; Lujanienė *et. al.*, 2010; Saberi *et. al.* 2010; Ghaffar *et. al.*, 2012; Galamboš, 2012; Yavari *et. al.*, 2011; Nilchi *et. al.*, 2012; Taşdelen *et. al.*, 2013; Caccin *et. al.*, 2013; Abbas, 2013; Ding *et. al.*, 2014; Kim *et. al.*, 2014; Awual *et. al.*, 2014; Rouquerol *et. al.*, 2014).

Recently, rice husk which is a type of agriculture waste is used as adsorbent media for adsorption process of many pollutants such as heavy metals (Abbas and Abbas (a), (b), (c) and (d),2013; Abbas and Abbas (a) 2014), dyestuffs (Abbas and Abbas (b), 2014), pesticides (Abbas and Abbas (c), 2014), phenols (Abbas *et. al.* (a), 2013) and non-organic toxins (Abbas *et. al.*, 2014) because it is available, very inexpensive and ability to remove different types of contaminants, thus the rice husk usage will decrease the cost of wastewater treatment considerably and would represent practical benefit of agriculture waste residue in disposal toxic matter in save way (Kim *et. al.*, 2013 and Kim *et. al.*, 2014).

Therefore, the aim of this study is to investigate the adsorption behaviour of cesium Cs^+ ion on rice husk from simulated synthetic aqueous solution (SSAS) similar to nuclear waste and utilize from the husk remaining in eco-friendly method.

2. Exprimental Work

2.1 Materials

2.1.1 Rice husk (adsorbent media)

Rice husk was collected from Al-Shanafia fields for rice in the

Southern of Iraq. The rice husk was washed three times with doubled distilled water. Excess distilled water was used to remove the soluble materials present in the rice husk bringing from the field, boiled to remove colour and other fine impurities may be found in the rice husk, and then dried at 105°C for 24 hours and the adsorbent thus processed was used in its original piece size. The surface area of RH was measured by BET (Brunauer – Emmett – Teller nitrogen adsorption technique). Characteristics of RH were presented in **Table 1**. When the RH was heated in an oven, most of the water had been removed from the rice husk while the second major mass loss of about 45-65% was attributed to the breakdown of cellulose constituent char, which is a carbonaceous residue.

Table1: Characterization properties of Iraqi rice husk

Compound	Composition wt %
SiO_2	90.70
Al_2O_3	0.13
Fe_2O_3	0.06
TiO_2	0.015
CaO	0.61
MgO	0.25
Na_2O	0.09
K_2O	2.64
P_2O_5	0.73
LOI	4.71
S.A (m^2/g)	17.5

2.1.2 Stock solutions

In order to avoid interference with other elements in wastewater, the experiments in this study were carried out using SSAS of different cesium concentrations. 1000 mg/l stock solution of cesium was prepared by dissolving known weight of cesium nitrate $CsNO_3$ in one litre of double distilled water, all solutions using in the experiments were prepared by diluting the stock solution with double distilled water to the desired concentrations for the experimental work of this investigation. The cesium concentrations were measured using spectrophotometer method using spectrophotometer thermo – genesys 10 UV, USA.

2.2 Batch adsorption experiments

The batch experiments were intended to test the removal cesium ion by adsorption technique through treat SSAS of cesium at desired concentration, various dosages of the RH (adsorbent media), different agitation speed and various pH. The pH value was adjusted using 0.1 N NaOH and 0.1 N HCl solutions. Batch sorption experiments were carried out using 100 ml glass bottles with addition of a known weight (1 g) of RH and (50 ml) of ^{137}Cs solution and shaken in a thermostat adjusted water bath shaker at different initial concentrations (C_o) from (1-100 mg.l^{-1}), different temperatures (25-45°C), different contact times (0.08-24 h), different agitation speed (100-400 rpm) and different pH (1-8). The cesium determination was carried out in atomic absorption spectrometer at a wavelength 852.1 nm. All experiments were triplicated to decrease the error. The amount adsorbed and percentage removal of cesium ion at the rice husk was determined using the following equations:

$$q = \frac{V}{w}(C_\circ - C_t) \qquad (1)$$

$$R = \frac{(C_\circ - C_t)}{C_\circ} \times 100 \qquad (2)$$

where q is the amount of cesium ions adsorbed onto RH (mg.g-1); $C_\circ$0 is the initial concentration of cesium ions (mg.l^{-1}) at $t = 0$; C_t is the concentration of cesium ions at $t = t$ (mg.l^{-1}); V is the initial solution volume (l); w m is the RH weight (g); and R is the percentage removal of cesium ion using IRH.

2.2.1 Adsorption Isotherms, Adsorption Kinetics and Adsorption Thermodynamics

2.2.1.1 Adsorption Isotherms

In general, the adsorption process is often evaluated by conducted the adsorption isotherms. The Langmuir, Freundlich, BET, Temkin and Dubinin-Radushkevich models are the most extremely used to describe the adsorption isotherms from experimental data. These models provide information to determine the removal efficiency of solute and an estimation of adsorbent amounts needed to remove solute ions from aqueous solution. Their mathematical expressions are listed in **Table 2**.

Table 2: The mathematical expressions of adsorption isotherm models

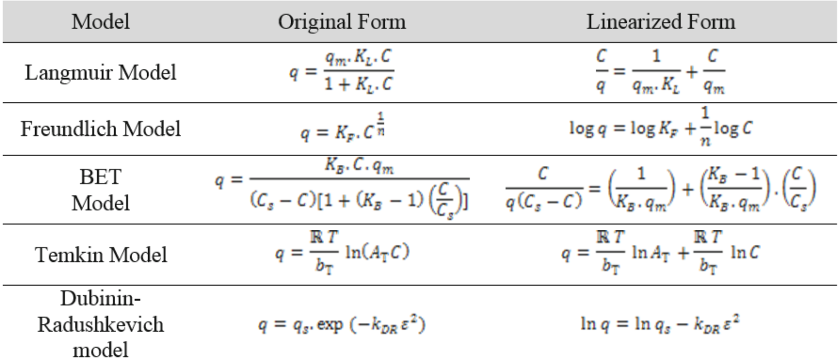

Model	Original Form	Linearized Form
Langmuir Model	$q = \frac{q_m . K_L . C}{1 + K_L . C}$	$\frac{C}{q} = \frac{1}{q_m . K_L} + \frac{C}{q_m}$
Freundlich Model	$q = K_F . C^{\frac{1}{n}}$	$\log q = \log K_F + \frac{1}{n} \log C$
BET Model	$q = \frac{K_B . C . q_m}{(C_s - C)[1 + (K_B - 1)\left(\frac{C}{C_s}\right)]}$	$\frac{C}{q(C_s - C)} = \left(\frac{1}{K_B . q_m}\right) + \left(\frac{K_B - 1}{K_B . q_m}\right) . \left(\frac{C}{C_s}\right)$
Temkin Model	$q = \frac{\mathbb{R} T}{b_T} \ln(A_T C)$	$q = \frac{\mathbb{R} T}{b_T} \ln A_T + \frac{\mathbb{R} T}{b_T} \ln C$
Dubinin-Radushkevich model	$q = q_s . \exp(-k_{DR} \varepsilon^2)$	$\ln q = \ln q_s - k_{DR} \varepsilon^2$

where:

$\boldsymbol{q}$ the adsorbed amount per adsorbent amount (ml.g^{-1}).

$\boldsymbol{q_m}$ the adsorbed amount required to form a monolayer.

$\boldsymbol{n}$ the Freundlich equilibrium constant that related to the intensity of adsorption.

$\boldsymbol{C}$ the concentration of adsorbed substance (ml.l^{-1}).

$\boldsymbol{C_s}$ the concentration of solute at the saturation of all layers (ml.l^{-1}).

$\boldsymbol{K_L}$ the Langmuir equilibrium constant (l. mg^{-1}).

$\boldsymbol{K_F}$ the Freundlich equilibrium constant that related to the total adsorption capacity (mg. g^{-1}).

$\boldsymbol{K_B}$ the BET constant.

$\mathbb{R}$ the universal gas constant = 8.314 J.mol^{-1}.K^{-1}

A_T the Temkin isotherm equilibrium binding constant (l/g).
b_T the Temkin isotherm constant.
q_s the theoretical isotherm saturation capacity (mg/g).
k_{DR} the Dubinin–Radushkevich isotherm constant ($mol^2.kJ^{-2}$).
ε the Dubinin–Radushkevich isotherm constant (potential energy).

$$\varepsilon = \mathbb{R}T \ln\left(1 + \frac{1}{C_e}\right) \tag{3}$$

In Dubinin-Radushkevich model the approach was usually applied to distinguish the physical and chemical adsorption of metal ions with its mean free energy, E per molecule of adsorbate (for removing a molecule from its location in the sorption space to the infinity) can be computed by the relationship:

$$E = \frac{1}{\sqrt{2\beta}} \tag{4}$$

where β is denoted as the isotherm constant.

From the Langmuir equation, a further analysis can be made on the basis of a dimensionless equilibrium parameter, R_L , also known as the separation factor. It is given by the expression:

$$R_L = \frac{1}{1 + K_L.C} \tag{5}$$

The value of R_L lies between 0 and 1 for favourable adsorption, R_L >1 represents unfavourable adsorption, R_L =1 represents linear adsorption and the adsorption process is irreversible if R_L = 0.

2.2.1.2 Adsorption Kinetics

The mechanism of adsorption onto an adsorbent can be described by several mathematical models. The parameters found in these expressions are important in water and wastewater treatment process design. The kinetics of cesium adsorption was analyzed using different kinetic models which were the pseudo first order, the pseudo second order, the simple Elovich model and the Intraparticle diffusion model **(Abd El-Latif and Elkady, 2011)**. Their mathematical expressions are listed in **Table 3**.

Table 3: The mathematical expressions of adsorption isotherm models

Model	Linearized Form
Pseudo first-order	$\ln(q_e - q_t) = \ln q_e - k_1 t$
Pseudo first-order	$\frac{t}{q_t} = \frac{1}{k_2 (q_e)^2} + \frac{t}{q_e}$
Elovich	$q_t = \left(\frac{1}{\beta}\right) \alpha\beta + \left(\frac{1}{\beta}\right) \ln t$
Intraparticle diffusion	$q_t = k_i (t)^{0.5} + I$

where:

q_e the adsorption capacities at equilibrium (mg.g^{-1}).

q_t the adsorption capacities at time ***t***, (mg.g^{-1}).

k_1 the pseudo first-order rate sorption constant (min^{-1}).

k_2 the pseudo second-order rate sorption constant (g.mg^{-1}.min^{-1}).

α the rate of chemisorption at zero coverage (mg.g^{-1}.min^{-1}).

β the extent of surface coverage and activation energy for chemisorption (g.mg^{-1}).

k_i the intra-particle diffusion rate constant.

2.2.1.3 Adsorption Thermodynamic

The activation energy for the adsorption systems of cesium ion removal using the RH is determined from the Arrhenius equation:

$$\ln k_2 = \ln A - \frac{E_a}{\mathbb{R}T} \qquad \textbf{(6)}$$

where A is the temperature independent factor (frequency factor) (g.mg^{-1}.min^{-1}); k_2 is the pseudo-second-order rate constant value for the cesium ions sorption, E_a is the activation energy in kJ/mol, T is the temperature in degree Kelvin and $\mathbb{R}$ is the universal gas constant that equal to 8.314 J/mol K. The activation energy (E_a) for the studied sorption system was determined from the slope and A from the intercept of the plot $(\ln k_2)$ vs. $(1/T)$.

The values of enthalpy (ΔH°) and entropy (ΔS°) of the adsorption process were calculated using the following equation (Al-Zboona *et. al.*, 2011)

$$\ln k_d = \frac{\Delta S^\circ}{\mathbb{R}} - \frac{\Delta H^\circ}{\mathbb{R}T} \qquad \textbf{(7)}$$

where T is temperature in Kelvin, and $\mathbb{R}$ is the gas constant.

(k_d) is Distribution coefficient and is represented a standard parameter in the assessment of the physiochemical behaviour of metal ion between solid and liquid phases. It can be used to evaluate the sorption and retention of the metal ion in RH. k_d was calculated using the following equation:

$$k_d = \frac{\textbf{Concentration of Cs}^+ \textbf{ ion adsorbed } (\textbf{mg.l}^{-1}) \times \textbf{V}}{\textbf{Concentration of Cs}^+ \textbf{ ion adsorbed } (\textbf{mg.l}^{-1}) \times w} \qquad \textbf{(8)}$$

$$k_d = \frac{\mathbf{V}}{w} \times \frac{(C_\circ - C_{eq})}{C_{eq}} \qquad \textbf{(9)}$$

where $\mathbf{V}$ is the volume of the solution (l) and w is the mass of RH (g).

But from **equation (1)** when time reach to equilibrium time, i.e. $t = t_{eq}$. Therefore

$$q_{eq} = \frac{V}{w}\left(C_{\circ} - C_{eq}\right) \tag{10}$$

Substituting **equation (10)** in **equation (9)** yield:

$$\therefore \boxed{k_d = \frac{q_{eq}}{C_{eq}}} \tag{11}$$

From **equation 6** when $(\ln k_d)$ vs. $(1/T)$ is plotted, the slope of the straight line will yield $(\Delta H^{\circ}/\mathbb{R})$ and an intercept will be $(\Delta S^{\circ}/\mathbb{R})$, thus ΔS° and ΔH° can be determined.

The change in Gibbs free energy $(\Delta G^{\circ})$was calculated using the following equation:

$$\Delta G^{\circ} = \Delta H^{\circ} - T\Delta S^{\circ} \tag{12}$$

2.3 Fixed bed adsorption experiments

Fixed bed column of continuous mode experiments were conducted in order to test cesium removal by treated SSAS of above cesium at desired concentration with the various bed heights of the adsorbent media RH using different flow rates of SSAS of cesium at various pH. The pH value was adjusted using 0.1 N NaOH and 0.1 N HCl solutions. The flow direction is downward by gravity. The sorption unit consists of two glass container of SSAS of cesium one for inlet and another for outlet each of (1 liter) capacity. Glass column has 2.54 cm ID and 150 cm height.

The sorption column packed with adsorbent media to a height of (10-100 cm) supported from the top and the bottom by glass hollow cylinder layer, each cylinder has (0.5 cm ID, 0.1 cm thickness and 1 cm long). Before starting the runs, the packed bed sorption column was rinsed by double distilled water down flow through the column. The RH is packed in the column to the desired depth, and fed to it as slurry by mixing the media RH with distilled water in order to avoid the formation of air bubbles inside the media. After the packed bed sorption column was accommodation and putting the required amount of adsorbent media, the adsorption process started by allowing the cesium SSAS of required concentration and pH down flow through the sorption column from inlet container by gravity at a precise flow rate in experiment which is adjusted by the valve. To determination the best operational conditions, the experiments were carried out at a temperature between (20-45)°C, various pH values which are (1-8) and initial feed concentrations of SSAS of different cesium which are between (1-100) mg/l each one alone and at different flow rates which are between (5-100) ml/min for cesium initial feed concentration. Outlet samples after treatment in each experiment were collected every 10 minutes from the bottom of packed column and the unadsorbed concentration of cesium in SSAS was analyzed spectrophotometrically.

3. Mathematical Model

Fixed bed dynamics are describing by a set of convection-diffusion equations, coupled with source terms due to adsorption and diffusion inside adsorbent particles. Inside the particle, molecules of adsorbate diffuse into the inner portions of particle via surface diffusion, pore diffusion, or both. The solution of these equations will give rise to the prediction of the needed concentration distribution. This investigation focuses on understanding the mechanism of both surface diffusion and pore diffusion. To formulate a generalized model corresponding to the dispersion flow, surface diffusion and pore diffusion mechanism, following assumptions are made:

1. The system operates under isothermal conditions.

2. The equilibrium of adsorption is described by Langmuir isotherm.
3. Intraparticle mass transport is due to Fickian diffusion, and it is characterized by the pore diffusion coefficient, and the surface diffusion,.
4. Mass transfer across the boundary layer surrounding the solid particles is characterized by the external-film mass transfer coefficient.
5. Film transfer resistance for mass transport from the mobile to the stationary phase.
6. Local adsorption equilibrium between the adsorbate adsorbed onto the adsorbent surface and the adsorbate in the intraparticle stagnation fluid.
7. Both surface and pore diffusion are included in the mass transport mechanism.
8. Axial dispersion.

3.1 Simulation Technique

Equations used in simulation technique represent a set of simultaneous, nonlinear, partial differential equations (PDEs) that can be solved numerically. The discretization was applied to space coordinates (Z and r) to convert the PODs to a set of ordinary differential equations (ODEs). The resulting ODEs can be solved using an existing ODE solver provided by MATLAB (Abbas and Abbas (a), (b), (c) and (d),2013).

4. Results and Discussion

4.1 Cesium ion removal using rice husk

The ability of RH to remove cesium from SSAS at various parameters which are pH of SSAS of cesium (*pH*), of adsorbent media RH bed height (*l*), flow rates of SSAS (*F*), SSAS temperature (T_{feed}) and time of treatment (*t*) was investigated. The experiments were achieved by varying all above parameters for different initial concentrations (C_o) of SSAS of cesium. Thus, the results obtained are explained below.

4.1.1 Effect of Initial Concentration

The effect of initial concentration on the adsorption of Cs^+ ions by RH is investigated employing different values ranging from 1-100 $mg.l^{-1}$. Result indicates that the adsorption efficiency decreases while initial concentration increases as shown in **Figure 1**. With low initial concentration, the available pores in the adsorbent surface are sufficient to adsorb most of the Cs^+ ions, which had filled the possible available sites, so the adsorption efficiency remains suitable to a low and moderate concentration. As the initial concentration increases, the available pores become insufficient to adsorb further metal ions and much of ions still in suspension and no Cs^+ ions can be adsorbed, therefore the percent removal was decreased with increasing initial concentration of cesium. For RH adsorbent media, higher percent removal were 95.70 % for cesium at initial cesium concentration of 1 mg/l, so RH was found to be efficient to cesium removal from SSAS and wastewater.

4.1.2 Effect of pH

The effect of SSAS initial pH on the adsorption of Cs^+ ions by RH is presented in employing different values ranging from 1-8. Result indicates that the adsorption efficiency increases while pH increases too as shown in **Figure 2**. At low pH values, there is an excess of hydronium ions H_3O^+ in the solution, these H_3O^+ions may be established bonds between hydronium ions and the surface of RH. Therefore, the positive surface charge will be formed and decreased the adsorption percentage of cesium ions on RH. Furthermore, a weak affinity toward RH can be attributed partly to the competition between the positively hydronium ion and Cs^+ ions. As the pH increases, the competition between protons and Cs^+ ions for surface sites will decrease and Cs^+ ions is the predominating species, which will attract to the surface of RH by columbic forces. As pH increases, the concentration of the hydronium ions, as competitors, decreases which leads to an increase of the amounts of adsorbed cesium and the acidic functional groups on RH are progressively deprotonated and the surface of RH become more negatively charged which causes a more electrostatic attraction of cesium (Yavari *et. al.*, 2011).

4.1.3 Effect of Adsorbent Media Bed Height

The effect of adsorption media of packed bed height on the adsorption of Cs^+ ions by RH is elucidated in employing different values ranging from 0.1-1 m. Result indicates that the adsorption efficiency increases while the packed bed height increases too as shown in **Figure 3**. The increased of bed height (*l*) meaning increased in the amount of adsorbent media RH, thus increasing the surface area of adsorbent material, hence increased the number of active sites in the adsorbent material surface i.e. increased the availability of binding sites for adsorption and consequently increase cesium removal capacity on RH. This lead to increase the ability of adsorbent media to adsorb greater amount of cesium from SSAS at different initial concentrations and ultimately the percent removal of cesium increased.

4.1.4 Effect of Flow Rate

The effect of SSAS flow rate on the adsorption of Cs+ ions by RH is evaluated in employing different values ranging from 5-100 $ml.min^{-1}$. Result indicates that the adsorption efficiency decreases while the flow arte (*F*) increases as shown in **Figure 4**. This may be due to the fact that when the flow of SSAS of cesium increased, the velocity of SSAS in the column packed with the adsorbent media RH was increased too, so the solution spend shorter time than that spend in the column while at low flow rate, and the SSAS of cesium resides in the column for a longer time, therefore undergoes more treatment with the adsorbent media, thus the adsorbent media uptake low amount of cesium from SSAS of cesium for high flow rate, therefore the percent removal of cesium was decreased when the flow rate was increased.

4.1.5 Effect of Feed Temperature

The effect of SSAS feed temperature on the adsorption of Cs^+ ions by RH is elucidated in employing different values ranging from 20-45°C. Result indicates that the adsorption efficiency increases while the feed temperature (T_{feed}) increases too as shown in **Figure 5**. The effect of temperature is fairly common and increasing the mobility of the Cs^+ ions. Furthermore, increasing temperatures may produce a swelling effect within the internal structure of the adsorbent media enabling cesium ions (Cs^+) to penetrate further (Abbas and Abbas (a), (b), (c) and (d),2013). Moreover elevating the curing temperature increases the extent and rate of reaction, shown through an increase in porous structure, surface area, and pore volume which enhance adsorption process. Additionally, at higher temperature an increase in active sites occurs due to bond rupture inside the specimen inasmuch of water vaporization and formation of micro-cavities thereby increases adsorption capacity (Al-Zboona *et. al.*, 2011).

4.1.6 Effect of Treatment Time

The effect of treatment time on the adsorption of Cs+ ions by RH is demonstrated in employing different values ranging from 10-60 min. Result indicates that the adsorption efficiency increases while the treatment time (t) increases too as shown in **Figure 6**. This may be due to the fact that when the treatment time of cesium SSAS increasing and the velocity of SSAS in the column packed with the adsorbent material was remaining constant, the solution spend longer time than that spend it when the time of treatment decreased, so the adsorbent material uptake more amount of cesium from SSAS, therefore the percent removal of cesium from SSAS was increased (Abbas and Abbas (a), (b), (c) and (d), 2013).

4.2 Adsorption Models

4.2.1 Adsorption Isotherms

The isotherm constants were calculated from the slopes and intercepts of **Figures (7-11)** and presented in **Table 4**. The value of R^2 was higher for Langmuir isotherm than the other isotherm model; that means Langmuir equation represented the adsorption process very well. Value of q_m, was calculated from the Langmuir plots. The maximum capacity of Rice Husk for cesium removal Cs^+ was calculated in the range of 2.0569 mg/g for initial concentration 1 mg/l at constant temperature that indicated the best adsorbing capacity of Rice Husk for cesium removal Cs^+. The equilibrium in the present investigation the equilibrium parameter was found to be in the range $0 < R_L < 1$ which is shown in **Table 4**. This indicated to the fact that the sorption process was very favourable and the adsorbent employed exhibited a good potential **(Abbas *et. al.*, 2013)**.

Table 4: Values of Langmuir, Freundlich, BET, Temkin and Dubinin–Radushkevich isotherm constants for the adsorption of cesium ion Cs^+ on rice husk at Optimum Conditions (C_o = 1 $mg.l^{-1}$, pH = 8, l = 1 m, F = 5 $ml.min^{-1}$, and T_{feed} = 45 °C)

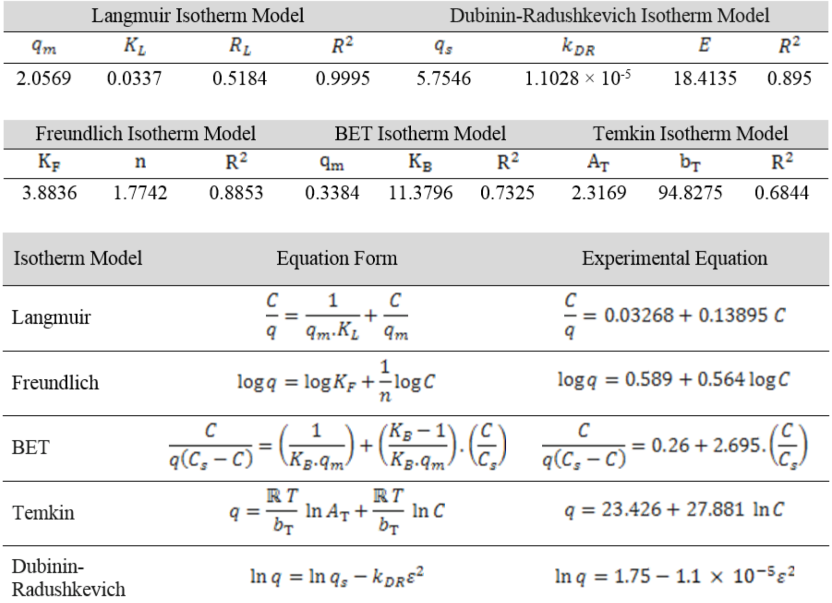

Langmuir Isotherm Model				Dubinin-Radushkevich Isotherm Model			
q_m	K_L	R_L	R^2	q_s	k_{DR}	E	R^2
2.0569	0.0337	0.5184	0.9995	5.7546	1.1028×10^{-5}	18.4135	0.895

Freundlich Isotherm Model			BET Isotherm Model			Temkin Isotherm Model		
K_F	n	R^2	q_m	K_B	R^2	A_T	b_T	R^2
3.8836	1.7742	0.8853	0.3384	11.3796	0.7325	2.3169	94.8275	0.6844

Isotherm Model	Equation Form	Experimental Equation
Langmuir	$\frac{C}{q} = \frac{1}{q_m . K_L} + \frac{C}{q_m}$	$\frac{C}{q} = 0.03268 + 0.13895\, C$
Freundlich	$\log q = \log K_F + \frac{1}{n} \log C$	$\log q = 0.589 + 0.564 \log C$
BET	$\frac{C}{q(C_s - C)} = \left(\frac{1}{K_B . q_m}\right) + \left(\frac{K_B - 1}{K_B . q_m}\right) . \left(\frac{C}{C_s}\right)$	$\frac{C}{q(C_s - C)} = 0.26 + 2.695 . \left(\frac{C}{C_s}\right)$
Temkin	$q = \frac{\mathbb{R} T}{b_T} \ln A_T + \frac{\mathbb{R} T}{b_T} \ln C$	$q = 23.426 + 27.881 \ln C$
Dubinin-Radushkevich	$\ln q = \ln q_s - k_{DR} \varepsilon^2$	$\ln q = 1.75 - 1.1 \times 10^{-5} \varepsilon^2$

4.2.2 Adsorption Kinetics

In order to determine the sorption kinetic models of cesium ion Cs^+ from SSAS, first order the pseudo first order, the pseudo second order, the simple Elovich model and the Intraparticle diffusion models were applied to the obtained data from experimental work. The calculations were conducted at optimum operation condition to find the best kinetic model. The adsorption kinetic constant and correlation coefficients of these models were calculated and given in **Figures (12-15)** and **Table 5**. Good correlation coefficients R^2 were observed indicating that cesium uptake process can be approximated with the pseudo second order kinetics model which has the best correlation coefficient among other adsorption kinetic models was 0.93.Thus, the pseudo second order kinetics was pathway to reach the equilibrium.

Table 5: Values of the pseudo first order, the pseudo second order, the simple Elovich model and the Intraparticle diffusion constants for the adsorption of cesium ion Cs^+ on rice husk at Optimum Conditions (C_o = 1 $mg.l^{-1}$, pH = 8, l = 1 m, F = 5 $ml.min^{-1}$, and T_{feed} = 45 °C)

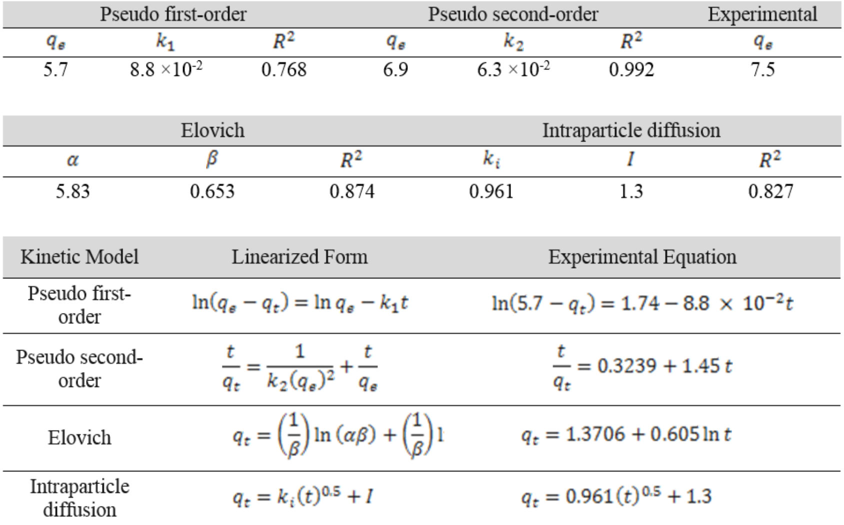

Pseudo first-order			Pseudo second-order			Experimental
q_e	k_1	R^2	q_e	k_2	R^2	q_e
5.7	8.8×10^{-2}	0.768	6.9	6.3×10^{-2}	0.992	7.5

Elovich			Intraparticle diffusion		
α	β	R^2	k_i	I	R^2
5.83	0.653	0.874	0.961	1.3	0.827

Kinetic Model	Linearized Form	Experimental Equation
Pseudo first-order	$\ln(q_e - q_t) = \ln q_e - k_1 t$	$\ln(5.7 - q_t) = 1.74 - 8.8 \times 10^{-2} t$
Pseudo second-order	$\frac{t}{q_t} = \frac{1}{k_2 (q_e)^2} + \frac{t}{q_e}$	$\frac{t}{q_t} = 0.3239 + 1.45\, t$
Elovich	$q_t = \left(\frac{1}{\beta}\right) \ln(\alpha\beta) + \left(\frac{1}{\beta}\right) \mathrm{l}$	$q_t = 1.3706 + 0.605 \ln t$
Intraparticle diffusion	$q_t = k_i (t)^{0.5} + I$	$q_t = 0.961 (t)^{0.5} + 1.3$

4.2.3 Adsorption Thermodynamic

Thermodynamics of Cs^+ adsorption on rice husk were studied at optimum operating condition values. Activation energy of cesium ions adsorption can be calculated from the slop of plotting $(\ln k_2)$ versus $(1/T)$ according to **equation (6)**. Uptake capacity (q) is calculated according to **equation (1)**, then **equation (7)** was used to determine energy parameters, where $(\ln k_d)$ was plotted against $(1/T)$, which results in a straight line and the values of enthalpy (ΔH°) and entropy (ΔS°) are obtained from the slope and intercept. The magnitude of the activation energy may give an idea about the type of adsorption. The relatively small value of the activation energy below 42 kJ/mol confirms the fact that the process of ion removal using the RH is diffusion controlled, i.e. the chemical step is much faster compared to mass transfer of ions inside the adsorption pores (Abd El-Latif and Elkady, 2011). ΔG° is calculated according to **equation (12)** as illustrated in **Figures (16** and **17)** and listed in **Table 6**.

The positive values of ΔH° and ΔS° and the decrease in the value of ΔG° with the increase in temperature show the adsorption process is an endothermic process and more favourable at higher temperatures. The endothermicity can be explained by the fact that the metals ions are well solvated and there is strong interaction between adsorbate and adsorbent. In order for metal ions to be adsorbed, they have to lose part of their hydration heat. This dehydration process of the metal ions requires energy. Endothermic nature of the system becomes dominant as the energy of dehydration supersedes the energy of the ions required to be attached on the surface. The positive value of ΔH° indicates that the entropy of the system increases after adsorption process which also supports the explanation the endothermicity process of the adsorption. When adsorption on RH occurs, the hydrated water molecules are separated from the metal ion before they attach to RH surface or penetrate into its structure, this will increase the disorder of the heterogeneous system and thus increases its entropy (Al-Zboona *et. al.*, 2011).

Table 6: Values of Enthalpy, Entropy, Gibbs Free Energy, Activation Energy and the Frequency Factor for the adsorption of cesium ion Cs^+ on rice husk at Optimum Conditions (C_o = 1 mg.l^{-1}, pH = 8, l = 1 m, F = 5 ml.min^{-1}, and T_{feed} = 45 °C)

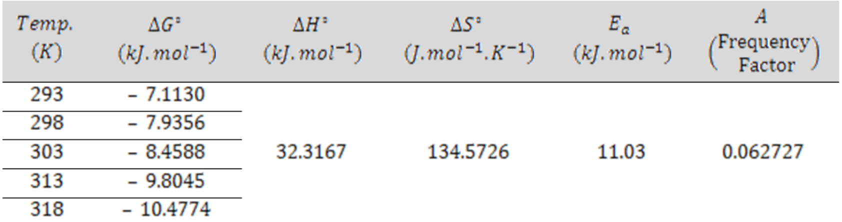

Temp. (K)	ΔG° ($kJ.mol^{-1}$)	ΔH° ($kJ.mol^{-1}$)	ΔS° ($J.mol^{-1}.K^{-1}$)	E_a ($kJ.mol^{-1}$)	A (Frequency Factor)
293	– 7.1130	32.3167	134.5726	11.03	0.062727
298	– 7.9356				
303	– 8.4588				
313	– 9.8045				
318	– 10.4774				

5. Profiting from Treated Rice Husk

5.1 Synthesis of promoted zeolite type Y catalyst from rice husk loaded with Cs^+ ions

Rice husk samples which were adsorbed cesium ions Cs^+ from aqueous solutions at different operating conditions was segregated and classified according to its contain of cesium and utilization from these samples as a raw material in synthesis of promoted catalyst and tested in n-heptane catalytic cracking which is zeolite type Y. The samples give different ratios of ***cesium ions Cs^+*** to ***rice husk***. The ratios were between (0.05 to 5.5 wt %). RH samples with different ratios were firstly treated with 10% phosphoric acid (H_3PO_4) for 24 hours for preliminary removing all impurities. Then they were well washed with double distilled water, filtered, dried in air, and calcined at 750°C for 6 hours. 12 g of calcined RH were then subjected for dissolution in sodium hydroxide NaOH (4 M) followed by refluxing at 90°C for 12 hours, then concentrated hydrochloric acid (HCl (37%)) was added to the aforementioned base dissolved RH to complete precipitation.

RH were filtered, washed with excess distilled water to be freeing from chloride ions and finally dried in an oven at 120°C for 6 hours. Zeolite type Y was synthesized using above prepared RH as a silica source in the following method. A 500 ml Teflon beaker containing a magnetic stirrer was washed with deionized water. Sodium hydroxide of 1.6616g was added slowly to deionized water and stir until clear and homogenous solution appeared for about 5 minutes. The aqueous solution of sodium hydroxide was ready for the preparation of seed gel. The gel was prepared according to the following molar chemical composition: **10.67 Na_2O: Al_2O_3: 10 SiO_2: 180 H_2O**. Two milliliter aqueous solution of sodium hydroxide was added to 0.7515g sodium aluminate oxide until a homogenous mixture was formed; 1.5361g of above prepared RH was added separately to 5.5 ml sodium hydroxide aqueous until homogenously mixed. Both of the preparations were heated under vigorous stirring to obtain a homogenous mixture. The sample was aged for 24 hours at room temperature in the Teflon bottle. The aluminate and silicate solutions were mixed together in the polypropylene beaker, subsequently stirred for 2 hours with the purpose of making it completely homogenized. This combined solution was used as the feed stock gel. The synthesized zeolite type Y which was in sodium (**Na^+**) powder form i.e. **Cs^+/NaY-Zeolite**, mixed with 15 % montmorillonite clay as a binder then mixed with water to form a paste. A spherical shape (0.5 cm) was formed, dried overnight at 110°C. In order to make a promoted catalyst ready for test in any process, hydrogen zeolite **(H-Zeolite)** form must be prepared.

The **Cs^+/HY-Zeolite** were prepared by exchanging Na^+ ions in the sodium form **(Cs^+/NaY-Zeolite)** with ammonium chloride solution NH_4Cl. In order to obtain ideal degree of ion exchange the technique of multi-steps (three times repeating) was used. Thus, the first step, 2 N of ammonium chloride solution (26.75 g of NH_4Cl in 250 ml of distilled water) contacted with 90 g of prepared **Cs^+/NaY-Zeolite** with stirring for 2 hours. In the second step, the procedure in the first step was repeated under the same conditions but on about 60 g of zeolite, which was taken from the total zeolite amount produced in the first step. Finally, in the third step, the procedure under the same conditions was repeated again but on about 30 g of zeolite, which was taken from the total zeolite amount produced in the second step. The exchanged ammonia zeolite were filtered off, washed with deionized water to be free of chloride ions dried overnight at 120^{o}C and then calcined initially at 150°C for two hours. The temperature was increased 75°C per hour until it reached 550°C and it was held constant for 5 hours at this temperature. During calcination, ammonia and water were liberated and promoted zeolite which is **Cs^+/HY-Zeolite** was formed (Abbas *et. al.* (b), 2013).

5.2 Synthesis of normally zeolite type Y catalyst from rice husk only

In the same way illustrated in above section exactly, normally zeolite type Y catalyst was prepared but the raw material was (normally RH) i.e. RH without treating with SSAS containing cesium ions Cs^+ (Abbas and Abbas (e), 2013).

5.3 Catalytic Activity of Synthesized Catalysts

The promoted and normally zeolite type Y catalyst activity was studied by applying n-heptane catalytic cracking reaction. The n-heptane catalytic cracking reaction was carried out in catalytic cracking unit. This unit is operated under atmospheric pressure and the experiments of catalytic cracking were performed in an experimental fluidized bed unit. The unit consists of n-heptane storage tank, gas flow meter, dosing pump, evaporator, condenser/separator, cooler with appropriate control, and power supply box. A suitable amount of zeolite type Y catalyst prepared from RH was charged in the reactor from the top of it. At preheating section, the feed was preheated at 400°C before entering to catalytic bed. The temperature controlled was setting at desired reaction temperature between (400-550°C) in the reaction zone.

The first condenser was supplied with water from chiller and second charged with ice. A suitable quantity of water was charged to the preheater to remove air from the reactor. This water changed to steam used for air stripping from the reactor. The temperature in preheater kept at 400°C. After stripping air from the reactor, the flow of water was stopped and began to n-heptane flow at a rate 4.5 ml/min to the reactor for ten minute period. The reaction products were flown through double pipe heat exchanger, internal tube ice bath, separation and collection for liquid storage, while the gaseous products passed through the liquid products and were collected in a vessel over water. The gas volume is determined by water displacement. A sample of gaseous product was collected and then analyzed by gas chromatography device (GC) (Dani, Model GC 1000 DPC), to determine the chemical composition of the gaseous product. Cracking liquid products also collected in a tube and then analyzed by gas chromatography, to determine the chemical composition of the liquids product. The catalyst was replaced after the end of each experiment. **Table 7** shows n-heptane catalytic cracking composition (Abbas, 2013).

6. Statistical Model

A statistical model was carried out to the experimental results obtained from this study. Regression analysis and **π** Theorem was adopted to maintain a relation between the percent removal of thorium and the feed temperature, flow rate, pressure, pH of feed solution, initial concentration of thorium, adsorbent media of BP bed height, treatment time, column diameter and other parameters. These relations are shown in **equation 13**, which has a correlation coefficient **(*R*^{2})** 0.99755.

$$\%R = 3.527 \times 10^{-7} \left(\frac{\rho_{sol}}{C_\circ}\right)^{0.227} . \left(\frac{l}{d}\right)^{0.28} . \left(\frac{T_f . Cp_{sol} . t}{\vartheta}\right)^{0.26} . \left(\frac{K_{sol} . T_f}{\gamma . u}\right)^{0.25} . (pH)^{0.0093} \quad (13)$$

where:		
	$\%R$	Percent Removal of Cesium ions from SSAS
	ρ	Density of SSAS, $(\mathrm{kg/m^3})$
	$C_\circ$	Initial Concentration of Thorium, $(\mathrm{kg/m^3})$
	l	Adsorbent Material Bed Height, (m)
	d	Internal Diameter of Sorption Column, (m)
	T_f	Feed Temperature, (K)
	$C_{P_{sol}}$	Heat Capacity of SSAS, (kJ/kg. K)
	t	Treatment Time, (s)
	ν	kinematic viscosity of SSAS, $(\mathrm{m^2/s})$
	K_{sol}	Thermal Conductivity of SSAS, (W/m.K)
	γ	Surface Tension, (N/m)
	u	Velocity of SSAS, (m/s)
	g	Acceleration of Gravity, $(\mathrm{m/s^2})$

Table 7: n-heptane catalytic cracking composition using prepared zeolite catalysts

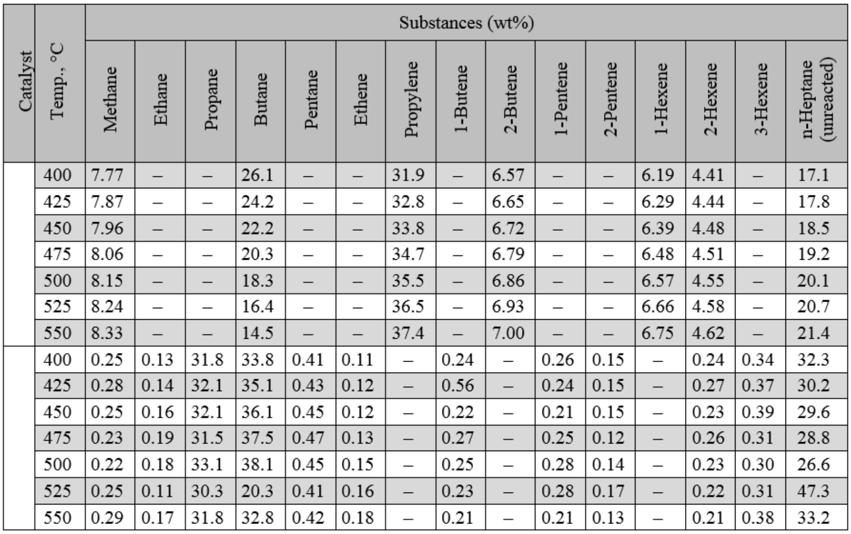

Catalyst	Temp., °C	Substances (wt%)														
		Methane	Ethane	Propane	Butane	Pentane	Ethene	Propylene	1-Butene	2-Butene	1-Pentene	2-Pentene	1-Hexene	2-Hexene	3-Hexene	n-Heptane (unreacted)
	400	7.77	–	–	26.1	–	–	31.9	–	6.57	–	–	6.19	4.41	–	17.1
	425	7.87	–	–	24.2	–	–	32.8	–	6.65	–	–	6.29	4.44	–	17.8
	450	7.96	–	–	22.2	–	–	33.8	–	6.72	–	–	6.39	4.48	–	18.5
	475	8.06	–	–	20.3	–	–	34.7	–	6.79	–	–	6.48	4.51	–	19.2
	500	8.15	–	–	18.3	–	–	35.5	–	6.86	–	–	6.57	4.55	–	20.1
	525	8.24	–	–	16.4	–	–	36.5	–	6.93	–	–	6.66	4.58	–	20.7
	550	8.33	–	–	14.5	–	–	37.4	–	7.00	–	–	6.75	4.62	–	21.4
	400	0.25	0.13	31.8	33.8	0.41	0.11	–	0.24	–	0.26	0.15	–	0.24	0.34	32.3
	425	0.28	0.14	32.1	35.1	0.43	0.12	–	0.56	–	0.24	0.15	–	0.27	0.37	30.2
	450	0.25	0.16	32.1	36.1	0.45	0.12	–	0.22	–	0.21	0.15	–	0.23	0.39	29.6
	475	0.23	0.19	31.5	37.5	0.47	0.13	–	0.27	–	0.25	0.12	–	0.26	0.31	28.8
	500	0.22	0.18	33.1	38.1	0.45	0.15	–	0.25	–	0.28	0.14	–	0.23	0.30	26.6
	525	0.25	0.11	30.3	20.3	0.41	0.16	–	0.23	–	0.28	0.17	–	0.22	0.31	47.3
	550	0.29	0.17	31.8	32.8	0.42	0.18	–	0.21	–	0.21	0.13	–	0.21	0.38	33.2

7. Conclusions

The following conclusions can be drawn:

1. RH showed a good ability to remove cesium from SSAS using adsorption technique. So, it could be recommended for removal of cesium from wastewater instead of other material because it is valid, cheaper, economical, and simplicity for using, and has a high ability to adsorb cesium, and can be used finally in another benefit use.
2. Maximum removal of thorium was 95.70% at initial cesium concentration of 1 mg/l.
3. The percentage removal of cesium was increased with decreeing flow rate of SSAS, and initial concentration of cesium while the percentage removal was increasing with increasing of pH, treatment time, temperature and the height of adsorbent material RH.
4. It can be prepared a catalyst promoter for cracking process of n-heptane from the residual samples of RH

that adsorb cesium from SSAS in catalytic cracking of n-heptane and remove the hazards radioactive waste in economic and eco-friendly method.

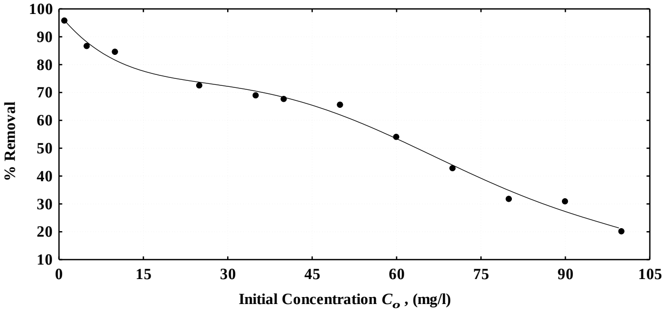

Figure 1: Effect of initial concentration ($C_\circ$) on the percentage removal of cesium @ *optimum conditions*

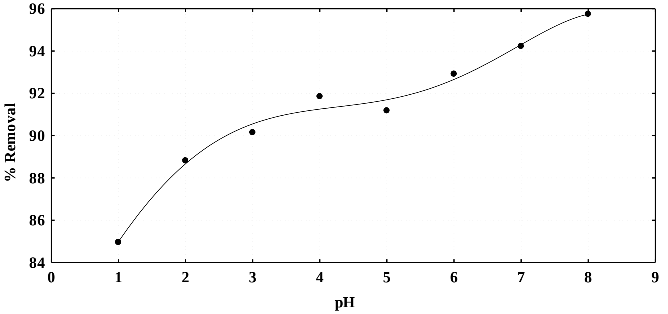

Figure 2: Effect of *pH* on the percentage removal of cesium @ *optimum conditions*

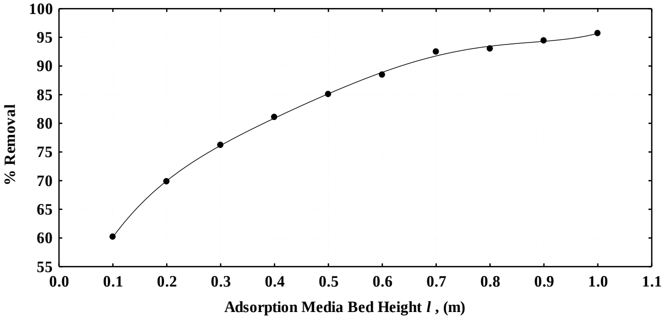

Figure 3: Effect of adsorption media bed height (*l*) on the percentage removal of cesium @ *optimum conditions*

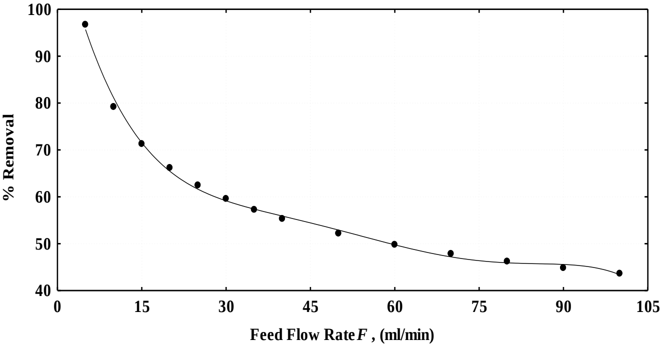

Figure 4: Effect of SSAS flow rate (*F*) on the percentage removal of cesium @ *optimum conditions*

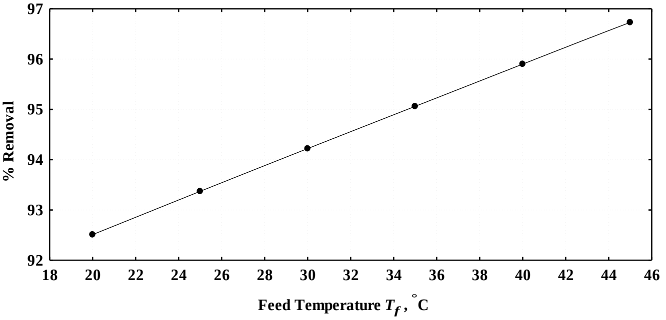

Figure 5: Effect of feed temperature (*T_f*) on the percentage removal of cesium @ *optimum conditions*

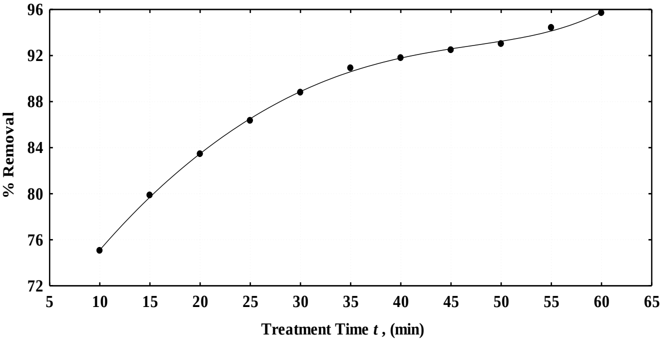

Figure 6: Effect of treatment time (*t*) on the percentage removal of cesium @ *optimum conditions*

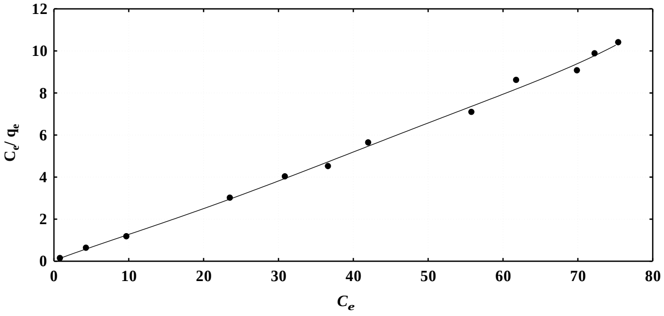

Figure 7 Langmuir adsorption isotherm model of cesium on RH @ optimum conditions

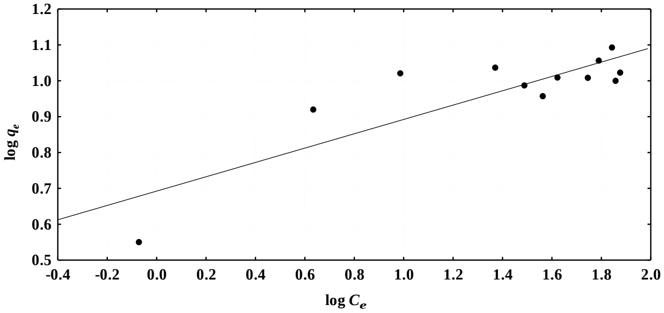

Figure 8 Freundlich adsorption isotherm model of cesium on RH @ optimum conditions

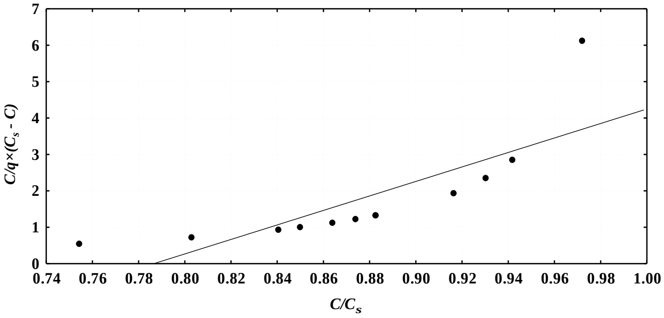

Figure 9 BET adsorption isotherm model of cesium on RH @ optimum conditions

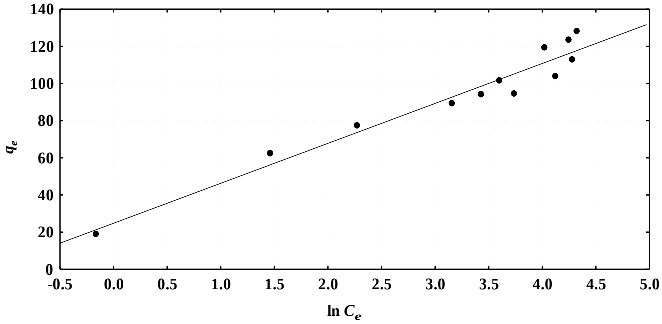

Figure 10 Temkin adsorption isotherm model of cesium on RH @ optimum conditions

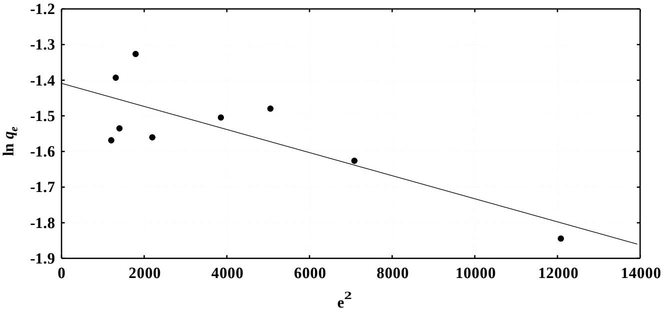

Figure 11 Dubinin-Radushkevich adsorption isotherm model of cesium on RH @ optimum conditions

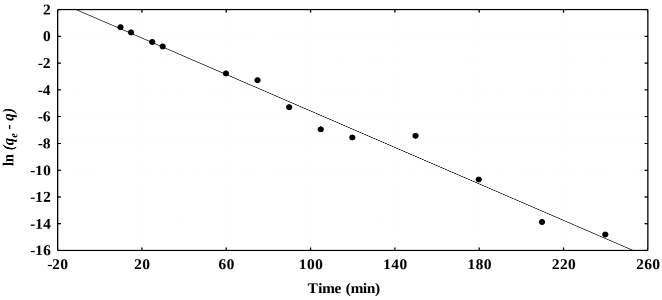

Figure 12 the pseudo first order kinetic model for adsorption of cesium ion @ optimum conditions

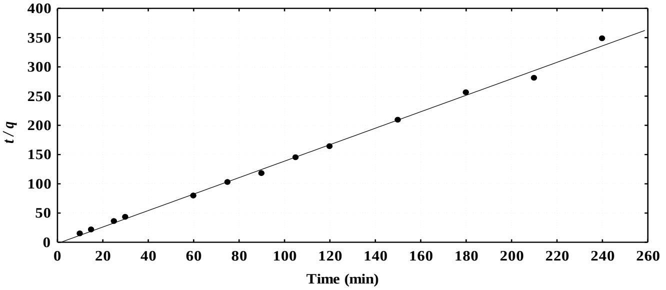

Figure 13 the pseudo second order kinetic model for adsorption of cesium ion @ optimum conditions

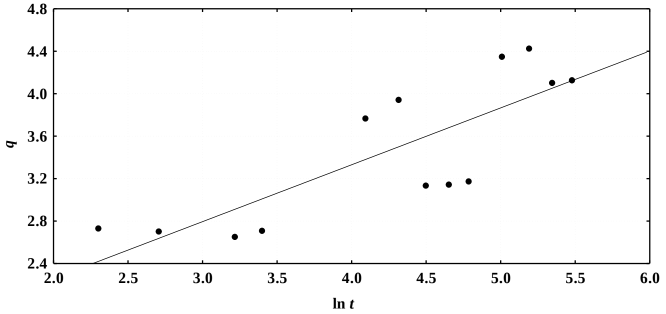

Figure 14 The Elovich kinetic model for adsorption of cesium ion @ optimum conditions

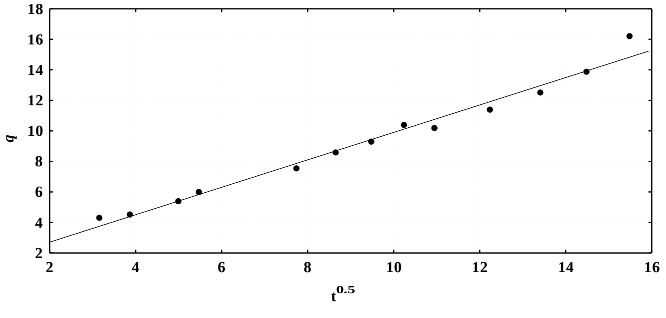

Figure 15 The Intraparticle diffusion kinetic model for adsorption of cesium ion @ optimum conditions

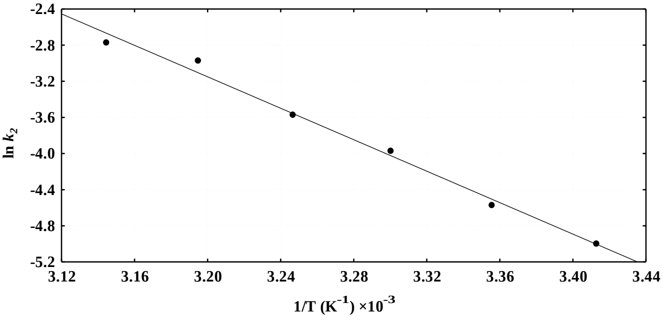

Figure 16 Arrhenius plots of Cesium removal using RH @ optimum conditions

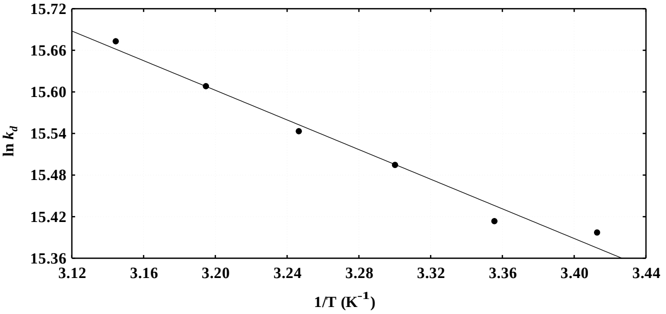

Figure 17 Effect of temperature on cesium kinetic adsorption using RH

BIBLIOGRAPHY

Abbas, F. S. 2013. "Thorium removal from waste water using Banana peel and employment of Waste Residue." *Advances in Natural and Applied Sciences* 7(3): 336-344.

Abbas, M. N., Abbas, F. S. and Ibraheem, S. A. 2014. "Removal of Cyanide Ion from Wastewater Using Banana Peel and Utilization from Residue." *Journal of Asian Scientific Research*: 637-154.

Abbas, M. N. and Abbas, F. S. 2013(a). "Iraqi Rice Husk Potency to Eliminate Toxic Metals from Aqueous Solutions and Utilization from Process Residues." *Advances in Environmental Biology* 7(2): 308-319.

Abbas, M. N. and Abbas, F. S. 2014(b). *Rice Husk as a Biosorbent Packed bed, Management, Utilization and Improvement compressive strength of concrete*. Germany: LAMBERT Academic Publishing.

Abbas, M. N. and Abbas F. S. 2014(c). *A Novel Method to Recycle the Treated Dye Wastes Adsorption, Exploitations and No Pollutants Remain*. Germany: LAMBERT Academic Publishing,

Abbas, M. N. and Abbas, F. S. 2013(d). "Utilization of Iraqi Rice Husk in the Removal of Heavy Metals from Wastewater." *Research Journal of Environmental and Earth Sciences* 5(7): 370-380.

Abbas, M. N. and Abbas, F. S. 2013(e). "The Predisposition of Iraqi Rice Husk to Remove Heavy Metals from Aqueous Solutions and Capitalized from Waste Residue." *Research Journal of Applied Sciences, Engineering and Technology* 6(22): 4237-4246.

Abbas, M. N. and Abbas, F. S. 2013(f). "The Feasibility of Rice Husk to Remove Minerals from Water by Adsorption and Avail from Wastes." *Research Journal of Applied Sciences*, WSEAS Transactions On Environment And Development 9 (4): 301.

Abbas, M. N., and Abbas F. S. 2013(g). *Manufacturing of Phenol using Reactive Distillation, Developing and Mathematical Analysis*. Germany: LAMBERT Academic Publishing.

Abbas, M. N., Abbas F. S., Nussrat H. H. and Hussein S. N. 2013. "Synthesis of Promoted Catalyst from Iraqi Rice Husk Used as a Raw Material for Treating Tannery Wastewater." *Australian Journal of Basic and Applied Sciences* 7(2): 511-528.

Abbas, M. N., Husain A. A. and Abbas F. S. 2013. "Phenol Removal from Wastewater Using Rice Husk." *Diyala Journal for Pure Sciences* 9(4): 51-60.

Abd El-Latif, M. M. and Elkady, M. F. 2011. "Kinetics study and thermodynamic behaviour for removing cesium, cobalt and nickel ions from aqueous solution using nano-zirconium vanadate ion exchanger." *Desalination* 271: 41–54.

Al Hamarneh, I., Wreikat, A. and Toukan, K. 2003. "Radioactivity concentrations of 40K, 134Cs, 137Cs, 90Sr, 241Am, 238Pu and 239+240Pu radionuclides in Jordanian soil samples." *J Environ Radio* 67: 53–67.

Al-Zboona, K., Al-Harahshehb, M. S. and Hania, F. B. 2011. "Fly ash-based geopolymer for Pb removal from aqueous solution." *Journal of Hazardous Materials* 188: 414–421.

Awual, Md. R., Suzuki, S., Taguchi, T., Shiwaku, H., Okamoto, Y. and Yaita, T. 2014. "Radioactive cesium removal from nuclear wastewater by novel inorganic and conjugate adsorbents." *Chemical Engineering Journal* 242: 127–135.

Bernatskii, D. P. and Pavlov, V. G. 2010. "Cesium adsorption induced inversion of the field electron emission from tungsten covered with nanostructural carbon." *Technical Physics Letters* 36 (7): 642-644.

Caccin, M., Giacobbo, F., Da Ros, M., Besozzi, L., and Mariani, M. 2013. "Adsorption of uranium, cesium and strontium onto coconut shell activated carbon." *Journal of Radioanalytical and Nuclear Chemistry* 297(1): 9-18.

Coplen, T. B. and Peiser, H. S. 1998. "History of the recommended atomic-weight values from 1882 to 1997: a comparison of differences from current values to the estimated uncertainties of earlier values." *Pure Applied Chemistry* 70(1): 237–257.

Cortés-Martínez, R., Olguín, M.T., and Solache-Ríos, M. 2010. "Cesium sorption by clinoptilolite-rich tuffs in batch and fixed-bed systems." *Desalination* 258: 164–170.

Danilin, L. D. and Drozhzhin, V. S. 2007. "Inorganic sorbents based on modified microspheres for treatment of liquid radioactive waste." *Radiochemistry* 49: 283–286.

Ding, D., Lei, Z., Yang, Y. and Zhang, Z. 2014. "Efficiency of transition metal modified akadama clay on cesium removal from aqueous solutions." *Chemical Engineering Journal* 236: 17–28

Galamboš, M., Magula, M., Daňo, M., Osacký, M., Rosskopfová, O. and Rajec, P. 2012. "Comparative study of cesium adsorption on dioctahedral and trioctahedral smectites." *Journal of Radioanalytical and Nuclear Chemistry* 293 (3): 829-837.

Ghaffar, A., Mazhar, F., Mashiatullah, A., and Alaamer, A. S. 2012. "A Modified Method for Removal and Stabilization of Cesium Metal in the Vitrified Matrix." *Journal of Water Chemistry and Technology* 34 (6): 258–263.

Inoue, K., Gurung, M., Adhikari, B. B., Alam, S., Kawakita, H., Ohto, K., Kurata, M., and Atsumi, K. 2014. "Adsorptive removal of cesium using bio fuel extraction microalgal waste." *Journal of Hazardous Materials* 271: 196–201.

Kim, C. K., Kong, J. Y., Chun, B. S., and Park, J. W. 2013. "Radioactive removal by adsorption on Yesan clay and zeolite." *Environ Earth Sci* 68: 2393–2398.

Kim, J. O, Lee, S.M., and Jeon, Ch. 2014. "Adsorption characteristics of sericite for cesium ions from an aqueous solution." *Chemical Engineering Research and Design* 92 (2): 368–374.

Lujanienė, G., Beneš, P., and Štamberg, K. 2010. "Effect of natural clay components on sorption of Cs, Pu and Am by the clay." *Journal of Radioanalytical and Nuclear Chemistry* 286 (2): 353-359.

Nilchi, A., Saberi, R., Moradi, M., Azizpour, H., and Zarghami, R. 2012. "Evaluation of AMP–PAN composite for adsorption of Cs+ ions from aqueous solution using batch and fixed bed operations." *Journal of Radioanalytical and Nuclear Chemistry* 292(2): 609-617.

Onishi, Y. 2014. "Fukushima and Chernobyl nuclear accidents' environmental assessments and U.S. Hanford Site's waste management." 23rd International Congress of Theoretical and Applied Mechanics, *Procedia IUTAM* 10: 372 – 381.

Pátzay, G., Weiser, L., Feil, F., Schunk, J. and Patek, G. 2009. "Radioactive wastewater treatment using selective ion exchangers." *Rperiodica polytechnica – Chemical Engineering* 53/2: 67–69. doi: 10.3311/pp.ch.2009-2.06.

Rogers, H., Bowers, J., and Anderson, D. G. 2012. "An isotope dilution–precipitation process for removing radioactive cesium from wastewater." *Journal of Hazardous Materials* 243: 124-129.

Rouquerol, J., Llewellyn, P., and Sing, K. 2014. "12 – Adsorption by Clays, Pillared Clays, Zeolites and Aluminophosphates." In *Adsorption by Powders and Porous Solids (Second Edition), Principles, Methodology and Applications,* 467–527.

Rowan, D. J. 2013. "Bioaccumulation factors and the steady state assumption for cesium isotopes in aquatic foodwebs near nuclear facilities." *Journal of Environmental Radioactivity* 121: 2–11, Special Issue: 2011 (ICRER meeting).

Saberi, R., Nilchi, A., Garmarodi, S. R., and Zarghami, R. 2010. "Adsorption characteristic of 137Cs from aqueous solution using PAN-based sodium titanosilicate composite." *Journal of Radioanalytical and Nuclear Chemistry* 284 (2): 461-469.

Sasaki, T., Okabe, J., Henmi, M., Hayashi, H., and Iida, Y. 2013. "Cesium (Cs) and strontium (Sr) removal as model materials in radioactive water by advanced reverse osmosis membrane." *Desalination and Water Treatment* 51: 1672–1677.

Sviridov, S. I., Tyurnina, Z. G. and Tyurnina, N. G. 2012. "Field-assisted diffusion of K+, Rb+, Cs+, Ag+, and Tl+ ions in sodium silicate glass." *Glass Physics and Chemistry* 38 (2): 206-211.

Taşdelen, B., Osmanlioglu, A. E. and Kam, E. 2013. "The adsorption behavior of cesium on poly(N-isopropylacrylamide/itaconic acid) copolymeric hydrogels." *Polymer Bulletin* 70 (11): 3041-3053.

Turekian, K.K. and Wedepohl, K. H. 1961. "Distribution of the elements in some major units of the Earth's crust." *Geological Society of America Bulletin* 72 (2): 175–192.

Yavari, R., Huang, Y. D., and Ahmadi, S. J. 2011. "Adsorption of cesium (I) from aqueous solution using oxidized multiwall carbon nanotubes." *J Radioanal Nucl Chem* 287: 393-401. DOI 10.1007/s10967-010-0909-6.